FRETTING WEAR OF T800 COATING IN AERO-ENGINE APPLICATIONS

Proceedings of ASME Turbo Expo 2020
Turbomachinery Technical Conference and Exposition
GT2020
September 21-25, 2020, Virtual, Online

GT2020-15608

FRETTING WEAR OF T800 COATING IN AERO-ENGINE APPLICATIONS

Mario Lavella[1], Daniele Botto[1]

[1]Department of Mechanical and Aerospace Engineering, Politecnico di Torino, Torino, Italy

ABSTRACT

High cycle fatigue in blades is triggered by oscillating forces. Devices such as shrouds, that exploit dry friction, are commonly introduced in the blade assembly to reduce the blade vibrations. If severe wear occurs, the effectiveness of the dry friction damping decreases, vibrations increase, and the number of cycles to failure of the blade diminishes. Mating surfaces in shrouds undergo high loads combined with relative displacement of low amplitude. This is the typical condition known as fretting. Coatings are commonly applied on damping surfaces of turbine blades to mitigate wear.

This study investigates the wear mechanism of contact interfaces coated by Tribaloy® T-800, a coating greatly used in aeroengines. The experimental campaign was performed with a point contact test rig. The investigation was carried out using as test parameters temperature, normal load and fretting amplitude. Nine sets of parameters were analyzed at different test durations. Friction coefficients were computed using the hysteresis loops measured during the fretting tests. The worn surfaces were measured by an optical equipment based on focus variation and the volume losses were accurately measured. The wear region was observed by scanning electron microscopy at the end of each test.

At room temperature, the friction coefficient was found substantially independent of the normal load. The wear rates at room temperature were higher than at high temperature. Observation of the worn surfaces by scanning electron microscopy revealed several brittle cracks. The damage mechanism changes from brittle (at room temperature) to ductile (at high temperature). The volume loss as a function of the dissipated energy was found independent of the normal load, showing that dissipated energy is a better variable rather than the number of wear cycles to show results of wear tests.

Keywords: Fretting, wear, friction, T800 coatings, turbine blades.

NOMENCLATURE

μ	friction coefficient
E_L	dissipated energy
N	normal force
T	tangential force
$S_{h,a}$	holes surfaces on the specific area a
$S_{p,a}$	peaks surfaces on the specific area a
$S_{h,w}$	holes surfaces on the worn area
$S_{p,w}$	peaks surfaces on the worn area
Δu	displacement amplitude
u	displacement
$V_{h,a}$	holes volume on the specific area a
$V_{h,i}$	holes volume on the unworn area
$V_{h,w}$	holes volume on the worn area
$V_{p,a}$	peaks volume on the specific area a
$V_{p,i}$	peaks volume on the unworn area
$V_{p,w}$	peaks volume on the worn area
V_w	wear volume of a contact surface

INTRODUCTION

Turbine disks in aeroengines are usually machined with slots - dovetail or firtree type - in which blades are fit in. In operating conditions, the centrifugal force pushes the blades against the disk slot and clamps the blade. Williams [1] presents a model of the blade dynamic based on a cantilever beam. It is common to equip blades with shrouds, usually placed at the tip of the blade. Each shroud is brought into contact with the shroud of the adjacent blades. Due to the characteristic geometry, this contact is sometime denoted to as z-notch. If a proper contact force is realized between the contact surfaces, condition that is usually achieved by twisting the blades, the stiffness of the assembly is increased. Increasing the stiffness of the assembly is beneficial to reduce the vibration amplitude of the blade and then to reduce the cumulative fatigue damage [2]. Similar devices that

use dry friction to damp vibrations are also applied to stators [3]. Contact surfaces, located at the blade attachment or at the tip shroud, undergo oscillating relative displacements caused by aerodynamic forces on the blade [4].

Contact pressure and relative displacement between the contact surfaces produce the typical phenomenon known as fretting. Fretting - whose most common consequences are wear, fatigue and corrosion - occurs on contact surfaces in relative reciprocating sliding motion of low amplitude with respect to the contact length along the sliding direction [5]. The amplitude of oscillations and the value of the contact pressure define the fretting regime [6]. If wear occurs, the contact surfaces at the tip shroud can lose press fit, the assembly becomes loose and the blade is free to vibrate under the external load. The fatigue loads acting on the blade, that was initially designed with constraints at the tip, are then increased, jeopardizing the safety of the whole disk. To reduce the amount of wear the designer can cover the contact surfaces with a low wear coating. Usually, coatings also diminish the friction coefficient. Root attachment of blades made with additive manufacturing are usually cover with coatings, to make up for the lack of wear resistance of components manufactured with this technology [7]. Special coatings have been developed to tolerate the high temperature during the operating conditions [8].

Tribaloy® T-800 is a widely used coating in aeroengine applications. Standard pin-on-disc or ball-on-disc wear tests on these coatings can be found in [9], [10]. These tests are not useful to characterize the fretting phenomenon occurring in aeroengines. In [11] is reported a comparison among T-800 and other coatings in terms wear-resistant coatings for use in high load applications. The oxidation behavior of the T-800 and its improvement is studied in [12], [13]. Corrosion resistance of Tribaloy ® T-400, T-401 and T-800 are compared in [14]. There is an evident lack in terms of fretting wear characterization of T-800 even though this coating is commonly applied on interfaces subjected to fretting.

The aim of this work is to study the fretting wear mechanism of Tribaloy ® T-800 under the typical operating conditions that can be found in blade attachment and z-notch. The coating was applied by plasma spray on specimens made of Inconel 718 superalloy. Tests were performed on an experimental setup designed and developed by the LAQ AERMEC laboratory of the Department of Mechanical and Aerospace Engineering of the Politecnico di Torino. Wear cycles were performed with different test conditions (normal loads, temperatures, wear cycles). Hysteresis cycles, namely the tangential contact force against the relative displacement, were measured throughout the experiment. Contact parameters (friction coefficient and contact stiffness) were extracted from the hysteresis cycles as function of wear cycles and dissipated energy. Before starting the test and at the end of the wear process, the three-dimensional topography of the mating surfaces was measured on each specimen. Comparison between the new and worn surface allowed loss volume estimation. Worm surfaces were also observed with a Scanning electron Microscopy (SEM).

1 Experimental device, test parameters and methodologies

The experimental campaign was performed using a fretting rig capable to test point contacts. In this rig a spherical surface, machined on the "spherical-surface" specimen, is pressed against a flat surface, machined on the "flat-surface" specimen. A flat and a spherical specimens makes the "tribo-couple". Tests were performed with different alternating relative displacement amplitude, normal load, and temperature at the frequency 100 Hz. The detailed experimental plan is displayed in TABLE 1. The "stroke" is the amplitude range of the relative displacement.

TABLE 1: EXPERIMENTAL PLAN PERFORMED AT ROOM TEMPERATURE.

Tribo couple ID	Substrate Material	Temp., °C	Stroke, µm	Normal Load, N	Cycles, $\times 10^6$
#01-01	CMSX4	600	30	32	3
#02-03	CMSX4	800	60	32	10
#03-06	Inconel 718	600	30	32	3
#04-01	Inconel 718	RT	150	12	5
#05-02	Inconel 718	RT	150	12	10
#06-03	Inconel 718	RT	150	12	15
#07-04	Inconel 718	RT	150	32	5
#08-05	Inconel 718	RT	150	32	10
#09-07	Inconel 718	RT	150	32	15
Temp.:	Temperature of the test				
RT:	Room Temperature, 24 C				
Frequency:	100 Hz				
Coating:	Tribaloy® T-800 applied by spray coating.				

Three parameters were chosen to define the test conditions: i) temperature, ii) normal load and iii) stroke. Nine combinations of these parameters were chosen among three temperatures (room temperature, 600 and 800°C), two normal loads (12 and 32 N) and three strokes (30, 60, 150 micrometers). Homologous Tribo-couples, in which specimens were made with the same bulk materials and coatings, were tested under the same test conditions but with different test durations, namely 3, 5, 10 and 15 10^6 wear cycles. The specimens were machined from a bar of CMSX4 or inconel 718 with a circular cross section and a diameter of 12 mm. A layer of 0.2 mm of T800 was applied on the contact surface of the specimen by spray coating.

FIGURE 1 illustrates the layout of the test rig. The constant normal load is applied to the spherical surface through dead weights. The flat surface was fit, through a support, on a vibrating beam. Oscillation of the beam generates the relative alternating motion of the flat surface with respect to the spherical surface, that is fixed to the ground. The support of the spherical-surface specimen is simply supported by two force sensors that measure the tangential contact force. The relative velocity of the two surfaces was measured as close as possible to the contact surfaces using two laser-doppler vibrometers, see FIGURE 2. In this way the relative displacement - computed by integration of the velocity – is not affected by any compliance of the test rig

[15]. This feature is not common in fretting test rigs where often a compliance between the contact surfaces and the measurement points affects the result. In the AERMEC fretting rig, the difference between the measured and the true displacement of the contact surfaces is negligible. The measured relative displacement was used as feedback signal to control the desired relative displacement amplitude.

An induction heating device is used to heat the specimens to a temperature up to 1000 °C. Temperature of the specimens is measured through a thermocouple inserted through the flat specimen beneath the contact point, see FIGURE 1b. The main characteristics of the test rig are summarized in TABLE 2, while a detailed description of this test rig can be found in [16].

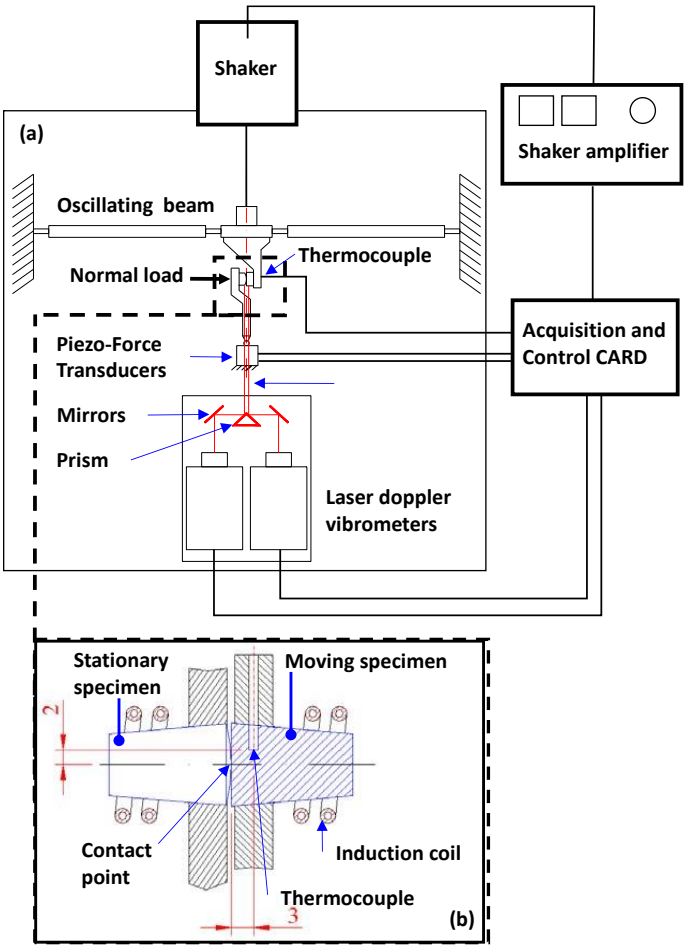

FIGURE 1: SKETCH OF THE TEST APPARATUS (a) WITH DETAIL OF SPECIMENTS (b).

TABLE 2: TEST RIG CHARACTERISTIC.

Normal load	10 ÷ 100	N
Displacement amplitude	0.5 ÷ 250	µm
Frequency	1 ÷ 150	Hz
Temperature	Up to 1000	°C

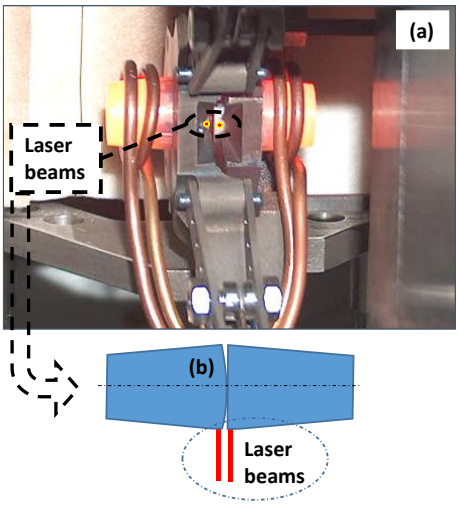

FIGURE 2: SPECIMENS ASSEMBLY (a) WITH ILLUSTRATION OF DISPLACEMENT MEASUREMENT SCHEME (a).

The friction coefficient µ (equivalent from the energy point of view) was computed using the hysteresis loops measured during the fretting tests

$$\mu = \frac{E_L}{4N\Delta u} \tag{1}$$

where N is the normal load, Δu is the maximum displacement amplitude of the hysteresis loop and E_L is the dissipated energy during the same hysteresis loop. The dissipated energy in one cycle comes from the integral of tangential force T over relative displacement u along the loop

$$E_L = \oint T\, du \tag{2}$$

The friction coefficient µ multiplied by the normal load gives the maximum tangential force, according to Amontons-Coulomb's law of friction, as it is applied to the entire stroke. If the micro-slip phase in the contact is negligible the friction coefficient µ computed with Eq.(1) is very similar to the friction coefficient determined in the standard way, namely dividing the friction force in gross slip conditions by the normal load. The friction coefficient µ is a little bit less than the friction coefficient obtained by the ratio tangential/normal forces.

The worn surfaces were measured by on optical 3D surface measurement system based on the focus variation principle. Volume losses, or wear volumes, were accurately computed with the procedure described in [17]. This procedure considers the effect of the roughness of contact surfaces on wear volume computation. According to this procedure a positive wear volume is produced if the volume of the peaks (peak volume) decreases and the volume of the holes (hole volume) increases. The wear volume (V_w) of one contact surface is then

$$V_w = (V_{p,i} - V_{p,w}) + (V_{h,w} - V_{h,i}) \quad (3)$$

where $V_{p,i}$ and $V_{h,i}$ stand for the sum of peaks and holes volumes in the initial unworn conditions respectively. Similarly $V_{p,w}$ and $V_{h,w}$ are the peaks and holes volumes of the worn regions respectively. The wear volume of one contact surface, the wear volume of a tribocouple is

$$V_{w,p} = V_{w,1} + V_{w,2} \quad (4)$$

where subscript 1 and 2 refer to the two contact surfaces. Volumes ($V_{p,i}$, $V_{h,i}$, $V_{p,w}$, $V_{h,w}$) are evaluated using the optical 3D surface measurement. Beforehand to compute the wear volume the non-flat surface needs a "form" removal. Form removal means that a macroscopic form is removed in order to take back to a macroscopic flat surface FIGURE 3(a), for example, a spherical surface is subtracted by the spherical contact surface. Topography of asperities and wear scar remain unaltered after the form removal process so that the volume loss measurements are not affected by this topological transformation. The surface to be subtracted from the measured surface was obtained by best fit interpolation of the unworn surface with the least square method. In other words, interpolation was performed using points outside of the worn region, see FIGURE 3. A reference plane was then defined by best fit interpolation with the least square method of the points outside the worn region. A reference plane is shown in FIGURE 3(b). At different stage of the wear process, the reference plane remain the same if it is based on the same unworn area (same interpolation points), see FIGURE 3(b). The peaks ($V_{p,i}$) and holes ($V_{h,i}$) volumes of the new surfaces are evaluated, before the wear process takes place, in the same area where the wear scar is expected to occur. This initial condition is important in mild-wear processes, because wear could result in only a small variation of the surface asperities. Obviously, for heavy wear the variation of the profile is much greater than the asperity dimensions and the initial volumes of peaks and holes can be neglected. If the measurement of peaks and holes volumes in unworn condition is not available, the initial peaks and holes volumes are evaluated using. Obviously, the area selected to evaluate initial peaks and holes volumes in unworn conditions must be as close as possible to the area of wear scar. Thus, the measurement of peaks and holes volumes needs to be applied to the real surface of the wear scar by means of a normalization. Let define the following volumes and areas,

- ($V_{p,a}$, $V_{h,a}$) the measured initial volumes of peaks and holes in the selected area;
- ($S_{p,a}$, $S_{h,a}$) the sum of surfaces of the peaks ($S_{p,a}$) and holes ($S_{h,a}$) measured on the reference plane and associated to the volumes ($V_{p,a}$, $V_{h,a}$) respectively;
- ($S_{p,w}$, $S_{h,w}$) the sum of surfaces of the peaks ($S_{p,w}$) and holes ($S_{h,w}$) measured on the reference plane and associated to the volumes ($V_{p,w}$, $V_{h,w}$) respectively.

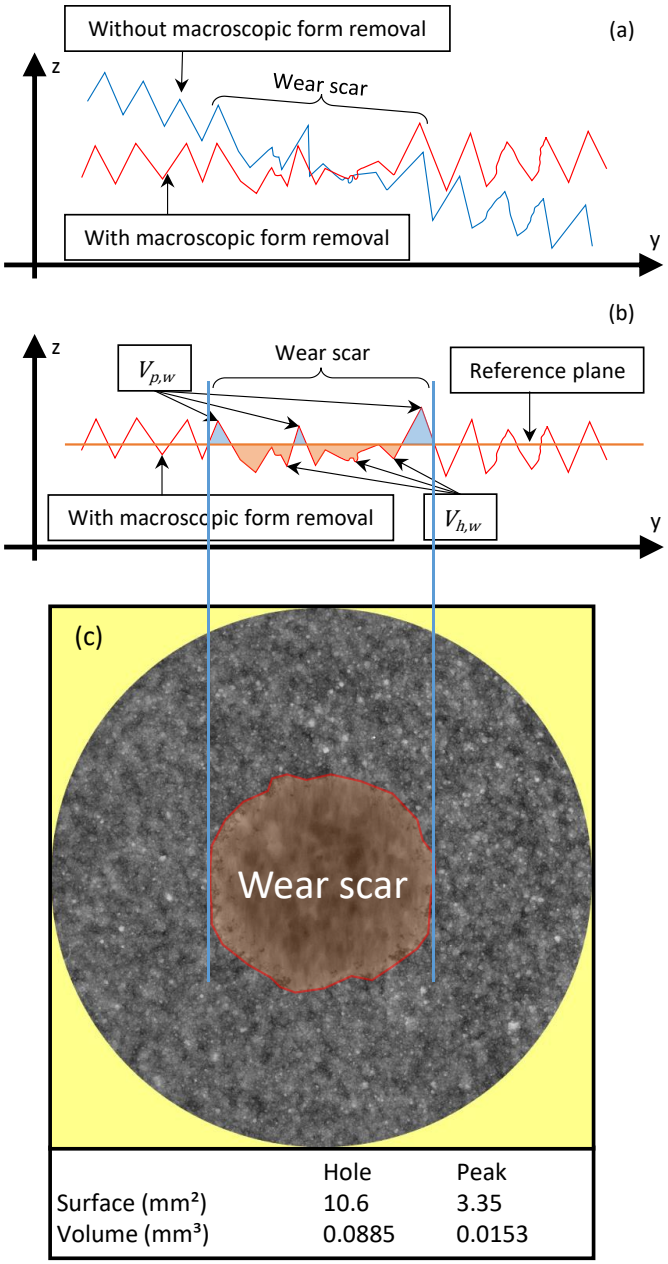

FIGURE 3: MACROSCOPIC FORM ROMOVAL (a); PEAK AND HOLE VOLUME MEASUREMNT (b); REFERENCE PLANE AND VOLUME OF PEAK AND HOLE (c).

The initial volumes of the peaks and holes in the area of the wear scar can be estimated by the following normalization of the reference measurements:

$$V_{p,i} = \frac{V_{p,a}}{S_{p,a}+S_{h,a}} S_{p,w} \quad (5)$$

$$V_{h,i} = \frac{V_{h,a}}{S_{p,a}+S_{h,a}} S_{h,w} \quad (6)$$

2 Results and discussion

The hysteresis loops were monitored continuously during the wear process. These loops were saved and stored when the target number of wear cycles was reached. FIGURE 4 reports the hysteresis loops measured at room temperature for two different normal loads in the initial and final stage of fretting process. As expected, the reported loops shows a lower area and friction force at lower normal load. With regard to the fretting process evolution, loops shows a stable shape and area. In other words, the contact seems to exhibit stable characteristic during the whole fretting process. Loops reported in FIGURE 4 illustrate a gross slip fretting regime that is stable during the entire fretting process. Analogous results in terms of the stability in shape and area of the hysteresis loop were found at high temperature in [16].

The friction coefficient was computed by post-processing the hysteresis loops according to Eq. (1). The friction coefficients as function of the fretting cycles is reported in FIGURE **5**. Each value of the friction coefficient is an average value obtained on a succession of 20 hysteresis loops. FIGURE **5** shows that the friction coefficient decreases drastically with the increasing of the temperature. A similar trend was found also for CERMET coating analyzed in [8]. FIGURE 6 shows the average friction coefficients, computed on each tribo-couple at room temperature, for different normal loads. As the variation of the friction coefficient with wear cycles is small the average is a good index to analyze the global trend.

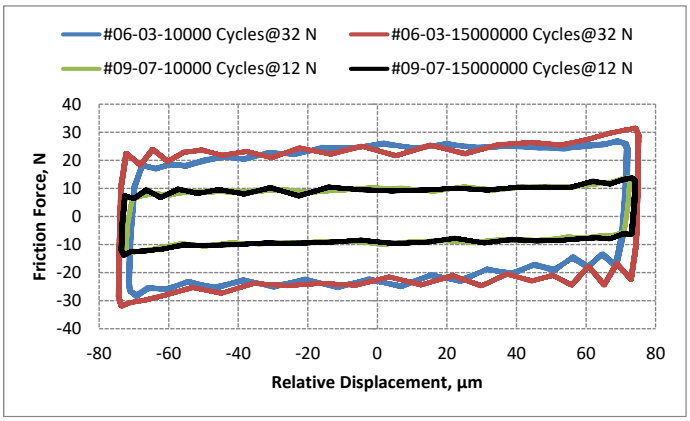

FIGURE 4: HYSTERESIS LOOP AT ROOM TEMPEMRATURE.

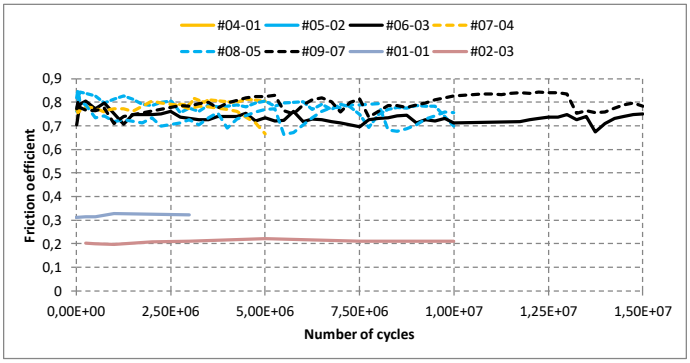

FIGURE 5: FRICTION COEFFICIENT AS A FUNCTION OF WEAR CYCLES.

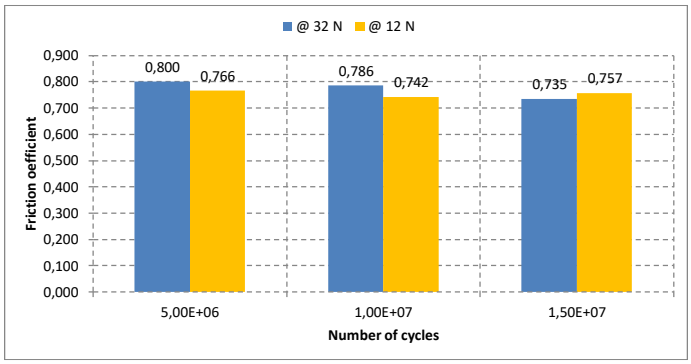

FIGURE 6: AVERAGE VALUE OF THE FRICTION COEFFICIENT AT ROOM TEMPERATURE FOR TWO NORMAL LOAD 31.8, 12.0 N.

TABLE 3 shows the average and standard deviation of all the friction coefficient measured during all the wear tests at room temperature for each normal load. Moreover, the average value computed on all fretting tests at room temperature is 0.76 with a standard deviation of 0.040. Based on the small difference between the average values can be concluded that the friction coefficients is independent of the normal load.

TABLE 3: AVERAGE FRICTION COEFFICIENT AS A FUNCTION NORMAL LOAD.

Normal load, N	Average friction coefficient	Standard deviation
12.0	0.77	0.043
31.8	0.76	0.037

The stability in shape and area of hysteresis loops during the evolution of the fretting cycles is confirmed by the stability of the friction coefficient and in general of the contact parameters. The stability property of loop seems to be independent of the bulk material (Inconel 718 rather than CMSX4), temperature (room temperature, 600 °C, 800 °C) and the stroke (30 µm, 60 µm, 150 µm). Moreover, FIGURE 5 revels that the friction coefficient is more stable at high temperature than at room temperature. This can be related with the softening effect at high temperature. The stability of the tangential contact stiffness was found in [16].

The wear volume as a function of the number of cycles and as a function of the dissipated energy is shown in FIGURE 7. The evolution of wear volumes with wear cycles at room temperature reveals a clear dependence on the normal load. Moreover, this evolution is linear at lower normal load while it is non-linear at high normal load. If the wear volume at room temperature is shown against the dissipated energy, the dependence on the normal load is included in the dissipated energy because the area of hysteresis loop is a function of the normal load [18]. Consequently, the wear volume-energy relationship at room temperature exhibits a linear trend for all energies excluded the highest (up to 75 KJ). At high dissipated energy the wear volume shows a sharply increase. In other

words, it seems that the wear volume shows a catastrophic evolution at high energy.

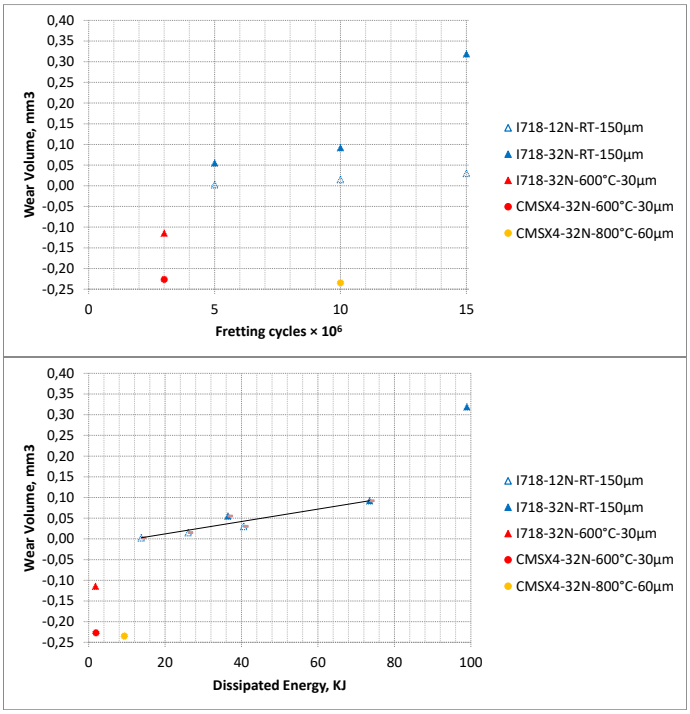

FIGURE 7: WEAR VOLUME AS A FUNCTION OF THE CYCLES AND DISSIPATED ENERGY.

At high temperature the evolution of wear volume reveals a negative value associate to the oxidation process. At 600 °C the oxidation process seems to be lower when the substrate is Inconel 718 than CMSX4. This can be interpreted as an effect of the higher softening property of the Inconel 718. The CMSX4 at 600 °C shows a lower decreasing of the elastic modulus and consequently a lower softening effect. Thus, it is probably that the higher stiffness of CMSX4 give origin to higher wear. This means higher volume of debris and consequently a more thick oxides layer.

Typical micrographs by Scanning Electron Microscopy (SEM) of the wear scar can be seen in FIGURE 8. These specimens were worn at the room temperature and at lowest number of cycles with the lowest normal load. The other specimens worn at room temperature show an analogous morphology while in [16] can be found typical SEM micrographs of the specimens worn at high temperature. As can be observed from FIGURE 8, the wear scar is completely full of brittle cracks. This seems to indicate that during the sliding the brittle cracks propagate up to generate wear debris. The dominant wear mechanism is abrasive in ploughing mode. At high temperature the behavior is more softening and consequently the wear mechanism is more ductile. Even if brittle fatigue cracks can be observed at high number of cycles [16] when the temperature increase a brittle-ductile transition could be expected.

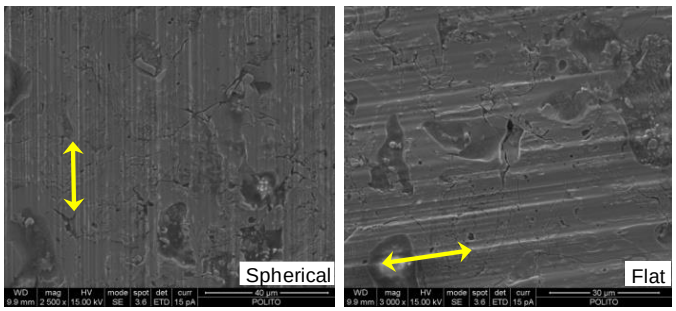

FIGURE 8: SEM MICROGRAPHS AT THE CENTRE OF WEAR SCAR OT THE COUPLE OF SPECIMENTS *#07-04.*

CONCLUSION

The point contact characterization by fretting wear experiments was performed on coating T-800 applied by plasma spray. Experiments were conducted with different sets of process parameters, namely three temperatures, three amplitudes, two normal loads, two substrates and different test durations.

At room temperature, the friction coefficient is independent of the normal load. The contact properties exhibit stable values independent of fretting cycles.

The SEM observation of the worn surfaces reveals a morphology of the wear scar completely covered with brittle cracks in each specimens fretted at room temperature. At this temperature, the dominant wear mechanism is abrasive in ploughing mode. On the other hand a more ductile behavior can be expected at high temperature. This could mean a brittle-ductile transition of wear mechanism. At high temperature, the more softening substrate exhibits a lower oxidation. The wear volume trend shows a catastrophic wear evolution at high dissipated energy while it shows a linear trend at lower dissipated energy. The wear process of T-800 at room temperature is much faster than the wear process at high temperature. This means that the fretting cycles at low temperature generate much more fretting damage than cycles at high temperature. Consequently, should be a good practice to count the number of fretting cycles that the turbine blade undergoes also at low temperature, e.g. before the blade reaches a thermal regime. Fretting wear cycles at low temperature could accelerate the fretting damage. Then they should be considered for a correct evaluation of the fretting damage. In order to increase the life of turbine blades the fretting cycles at low temperature should be avoided or limited, e.g. with a low rotation speed up to when the thermal regime is reach.

REFERENCES

[1] Williams, D. “Method of damping out bending vibrations of beam-like structures by dry (or coulomb) friction.” *Proc. Inst. Mech. Eng. Part C-J. Eng. 2* (1960) pp. 77–87.

[2] Firrone, C.M., Battiato, G. “A Reliable Pre-Processing for the Simulation of Friction Joints in Turbomachineries and its Validation: A Case Study With Policontact.” Proceedings of the ASME Turbo Expo. GT2019-91764. Phoenix, Arizona, USA June 17–21, 2019. DOI 10.1115/GT2019-91764.

[3] Battiato, G., Firrone, C.M. “A modal based reduction technique for wide loose interfaces and application to a turbine stator.” Mechanical Systems and Signal Processing (2019). DOI: 10.1016/j.ymssp.2019.106415
[4] Lassale, M., Firrone, C.M. “A parametric study of limit cycle oscillation of a bladed disk caused by flutter and friction at the blade root joints.” J. Fluids Struct. 76 (2018): pp. 349-366. DOI: 10.1016/j.jfluidstructs.2017.10.004.
[5] Lavella, M. “Partial-gross slip fretting transition of martensitic stainless steels” Tribology International 146 (2020). DOI: 10.1016/j.triboint.2020.106163.
[6] Vingsbo, O., Söderberg, S. “On fretting maps”, Wear 126 (1988): pp. 131–147.
[7] Lavella, M., Botto D. “Fretting Fatigue Analysis of Additively Manufactured Blade Root Made of Intermetallic Ti-48Al-2Cr-2Nb Alloy at High Temperature”, Materials 11(7) (2018): pp. 1152
[8] Botto, D., Lavella, M. “High temperature tribological study of cobalt-based coatings reinforced with different percentages of alumina.” Wear 318 (2014) pp. 89–97. DOI: 10.1016/j.wear.2014.06.024
[9] Navas, C., Cadenas, M., Cuetos, J.M., de Damborene, J. “Microstructure and sliding wear behaviour of Tribaloy T-800 coatings deposited by laser cladding.” Wear 260 (2006): pp. 838–846.
[10] Tobar, M.J., Amado, J.M., Álvarez, C., García, A., Varela, A., Yáñez, A. "Characteristics of Tribaloy T-800 and T-900 coatings on steel substrates by laser cladding." Surf. Coat. Technol. 202 (2008): pp. 2297-2301.
[11] Rao, J, Rose, T, Craig, M, Nicholls, J.R. “Wear Coatings For High Load Applications” Procedia CIRP 22 (2014) pp. 277-280.
[12] Zhang, Y.-D., Yang, Z.-G., Zhang, C., Lan H. "Oxidation Behavior of Tribaloy T-800 Alloy at 800 and 1,000 °C." Oxid Met 70 (2008): pp. 229-239.
[13] Zhang, Y.-D., Zhang, C., Lan, H., Hou, P.Y., Yang Z.-G. " Improvement of the oxidation resistance of Tribaloy T-800 alloy by the additions of yttrium and aluminium." Corrosion Science 53 (2011): pp. 1035-1043.
[14] Yao, M.X., Wu, J.B.C., Liu, R. " Microstructural characteristics and corrosion resistance in molten Zn–Al bath of Co–Mo–Cr–Si alloys." Materials Science and Engineering A 407 (2005): pp. 299–305.
[15] Fouvry, S., Kapsa, P., Vincent, L. “Analysis of sliding behavior for fretting loadings: determination of transaction criteria.” Wear 185 (1995): pp. 35–46.
[16] Lavella, M., Botto, D. "Fretting wear characterization by point contact of nickel superalloy interfaces." Wear 271 (2011): pp. 1543-1551. DOI 10.1016/j.wear.2011.01.064
[17] Lavella, M. “Contact Properties and Wear Behaviour of Nickel Based Superalloy René 80” Metals 6 (7) (2016): pp. 159. DOI: 10.3390/met6070159.
[18] Lavella, M., Botto, D. “Fretting wear of alloy steels at the blade tip of steam turbines.” Wear 426-427, (2019) pp. 735–740. DOI: 10.1016/j.wear.2019.01.039